

The Singlet-Triplet Jahn-Teller Polar Centers in Copper Oxides

A.S. Moskvin, Yu.D. Panov

Department of Theoretical Physics, Ural State University,
620083, Lenin Ave. 51, Ekaterinburg , Russia

E-mail: alexander.moskvin@usu.ru

Received January 20, 1998

Accepted February 4, 1998



Volume 2
No. 1, 1998

Abstract

One of the most exciting features of the hole centers CuO_4^{5-} in doped cuprates is in their unusually complicated ground state as a result of electronic quasi-degeneracy. An additional hole, doped to the basic CuO_4^{6-} cluster with the b_{1g} hole can occupy both the same hybrid $Cu3d-O2p$ orbital state resulting in a Zhang-Rice singlet $^1A_{1g}$ and the purely oxygen e_u molecular orbital resulting in singlet or triplet $^{1,3}E_u$ term with the close energies. We present a detailed analysis of the (pseudo)-Jahn-Teller effect driven by the near-degeneracy within the $^1A_{1g}, ^{1,3}E_u$ -manifold.

PACS : 71.27.+a, 74.20.s, 74.25.Ha, 76.60.-k

Keywords : cuprates, spin fluctuations, hyperfine coupling, nuclear resonance

Selected for publication by Programme Committee of youth scientific school "Actual problems of a magnetic resonance and its applications: Magnetic resonance in high T_c materials", Kazan, November 20-22, 1997

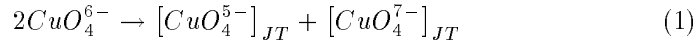
1 Introduction.

Unconventional properties of the oxides like $YBa_2Cu_3O_{6+x}$, $La_{2-x}Sr_xCuO_4$, $(K, Ba)BiO_3$, $La_{1-x}Sr_xMnO_3$, $La_2CuO_{4+\delta}$, $La_2NiO_{4+\delta}$ including systems with the high- T_c superconductivity and colossal magnetoresistance reflect a result of the response of the system to the nonisovalent substitution that stabilizes phases providing the most effective screening of the charge inhomogeneity. These phases in oxides may involve novel unconventional molecular cluster configurations like the Jahn-Teller sp -center [1] with anomalous high local polarizability and multi-mode behavior.

The numerous experimental investigations show that the origin of the high- T_c -superconductivity and of the other unconventional physical properties of the copper oxides are connected with an active interplay of the whole set of the degrees of freedom including the charge, spin, orbital and structural modes under conditions of the strong charge inhomogeneity and granularity.

Indirectly this is corroborated by the failures to explain more or less consistently the unconventional behavior of copper oxides as homogeneous systems within the "single-mode" scenarios such as the spin-fluctuation, electron-phonon or purely electronic ones.

An active interplay of the whole set of the modes is a natural element of the "multi-mode" scenario based on the so called "polar Jahn-Teller center model" proposed by the one of the authors earlier [1, 2, 3]. The CuO_4 -clusters based copper oxides in this model are considered as systems unstable with respect to the disproportionation reaction



with a formation of the system of the polar (hole - CuO_4^{5-} or electron - CuO_4^{7-}) pseudo-Jahn-Teller (PJT) centers. These centers are distinguished by the so called local S -boson or two electrons paired in the completely filled molecular orbital of the CuO_4 -cluster. In other words, the novel phase can be considered as a system of the local spinless bosons moving in the lattice of the hole PJT-centers $[CuO_4^{5-}]_{JT}$ or the generalized quantum lattice bose-gas (or liquid) with the boson concentration near $N_B = 1/2$.

Below we consider in more details a vibronic structure of the isolated PJT centers with taking account of some effects associated with spin-orbital coupling.

2 Correlations and the near degeneracy effects for the CuO_4 -clusters.

At first sight an analysis of the electronic structure and of the energy spectrum of the parent compounds such as $La_{2-x}M_xCuO_4$, $YBa_2Cu_3O_{6+x}$ at $x = 0$ does not display any exotic peculiarities except quasi two-dimensional antiferromagnetism determined by the strong exchange interaction for the $b_{1g}(d_{x^2-y^2})$ -holes

in the "basic" CuO_4^{6-} -clusters. At the same time it is worth to pay attention to one important feature namely to the exciton-band form of the fundamental absorption in the $1.5 \div 3.0$ eV region strictly pronounced in the systems like R_2CuO_4 , $YBa_2Cu_3O_{6+x}$, CuO [3].

A peculiar character of this absorption connected with the allowed charge-transfer transition $b_{1g} \rightarrow e_u$ between the copper-oxygen b_{1g} -hybrid and the purely oxygen e_u -orbital evidences the strongly correlated nature of the e_u -electrons with formal emergence of two types of the e_u -states with and without strong correlation. This peculiarity is connected with the maximal hole density occurred for oxygen ions just in the e_u -states of the CuO_4 -cluster and can be easily explained in the framework of the non-rigid anionic background model [4]. This model introduces new correlation degree of freedom with two possible states of anionic background for the valent $O2p$ -holes corresponding to two possible projections of the correlation pseudospin $s = 1/2$ and is described by the simplified Hamiltonian

$$H_{corr} = V_1 \hat{\sigma}_x + V_3 \hat{\sigma}_z \quad (2)$$

where $V_{1,3}$ are two operators acting within the valent states. Simple approximation used in [4] conjectures the linear n_{2p} -dependence for $V_{1,3}$ where n_{2p} is the $O2p$ -hole number. According to the optical data [3] the correlation pseudospin splitting can achieve the value ~ 0.5 eV.

An increase in the $O2p$ -hole concentration with the hole doping $CuO_4^{6-} \rightarrow CuO_4^{5-}$ results in sharp increase of the e_u -correlation splitting in the hole CuO_4^{5-} -centers with transformation of the $b_{1g} \rightarrow e_u$ fundamental band to the high-energy ($b_{1g}^2 \rightarrow b_{1g}e_u$) subband and the low-energy $b_{1g}^2 \rightarrow b_{1g}^*e_u^*$ subband to be well known as MIR (mid-infrared) absorption band [2].

Fig.1 shows qualitatively the results of the taking account of the considered " e_u -correlations" for the energy spectrum of the basic CuO_4^{6-} -cluster and the hole CuO_4^{5-} -cluster. It is important to mention an appearance in our model two types of the orthogonal (!) molecular orbitals, for instance b_{1g} (upper correlation sublevel) and b_{1g}^* (lower correlation sublevel) states, e_u and e_u^* .

Thus we come to a conclusion about a near-degeneracy for two configurations b_{1g}^{*2} and $b_{1g}^*e_u^*$ with b_{1g}^* and e_u^* being a lowest correlation sublevels. This result does not drastically change with taking into account an electrostatic interaction V_{ee} between two holes. Moreover, just the V_{ee} contribution was considered earlier [2] as a main reason of a near degeneracy for $^1A_{1g}$ (Zhang-Rice singlet) and $^{1,3}E_u$ -terms formed by b_{1g}^{*2} and $b_{1g}^*e_u^*$ -configurations. So, the both correlation effects lead to a near degeneracy in the ground state of the hole center CuO_4^{5-} .

Unusual properties of the ($^1A_{1g}, ^{1,3}E_u$)-manifold involving terms distinguished by the spin multiplicity, parity and orbital degeneracy provides unconventional behavior for the hole center CuO_4^{5-} with active interplay of various modes. As an extremely important result let note that E_u -doublet has a nonquenched Izing like orbital moment that can be directed only along the C_4 -axis.

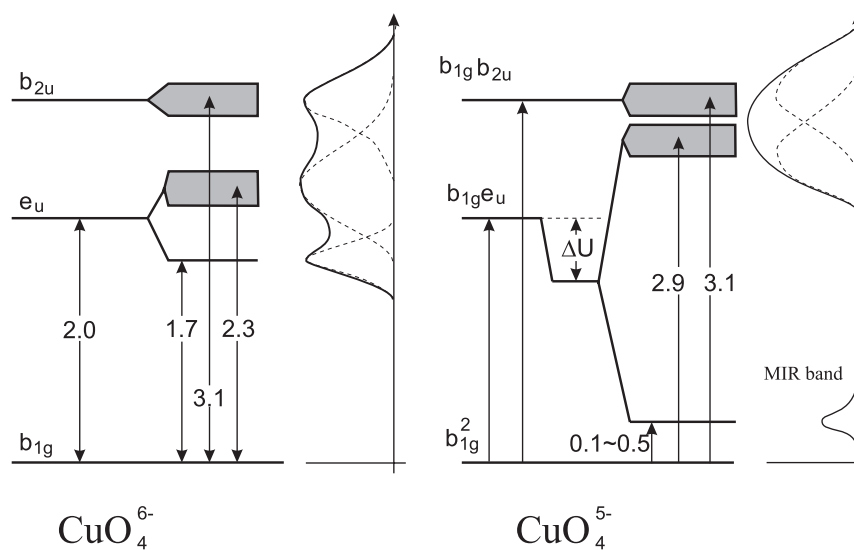


Figure 1: Correlation effects in the energy spectrum of the basic CuO_4^{6-} cluster and the hole CuO_4^{5-} center with numerical values (in eV) typical for oxides like CuO . On the right hand side we show a formation of the fundamental absorption spectra for the parent and hole doped oxides with peculiar MIR band in the latter case.

A near degeneracy within (${}^1A_{1g}, {}^{1,3}E_u$)-manifold can create conditions for the pseudo-Jahn-Teller effect [5] with anomalously strong electron-lattice correlations with the active local displacements modes of the Q_{e_u} -, $Q_{b_{1g}}$ - and $Q_{b_{2g}}$ -types.

3 Vibronic coupling for the CuO_4^{5-} centers.

3.1 The adiabatic potential.

Below we'll make use a notation $|SM_S, \gamma\rangle$ for the basis wave functions from the (${}^1A_{1g}, {}^{1,3}E_u$)-manifold (see Fig.2). Here, S ($= 0, 1$), M_S are the total spin and its projection, γ ($= A_{1g}, E_u^x, E_u^y$) are symbols of the irreducible representation of the symmetry group D_{4h} for the CuO_4 center and its row, respectively, which indicate the transformation properties of the orbital functions. Subsequently, we restrict ourselves with the linear vibronic coupling within the (${}^1A_{1g}, {}^{1,3}E_u$)-manifold with the JT-active vibrational coordinates of the a_{1g} , b_{1g} , b_{2g} , e_u symmetry.

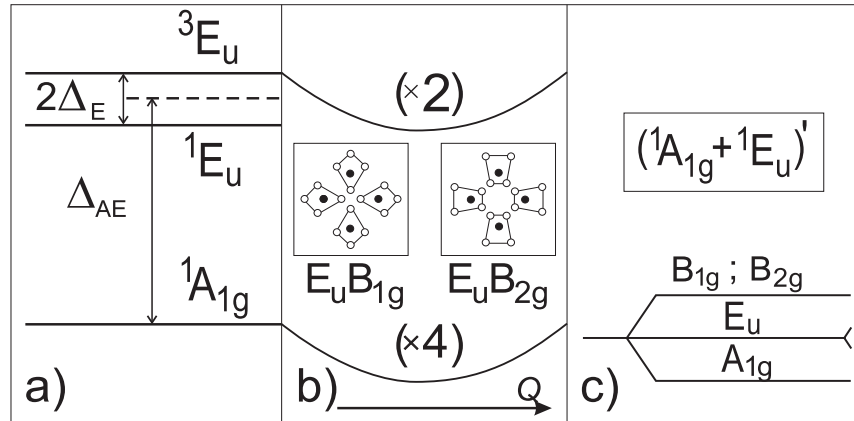


Figure 2: An illustration of the initial (a) CuO_4^{5-} -center energy spectrum modification with taking into account the strong Jahn-Teller pseudo-effect (b) and the tunnel splitting of the ground vibronic states (c). Corresponding to different minima of AP distortions are shown in insert.

Vibronic coupling for the isolated singlet or triplet ${}^{1,3}E_u$ -term has a well known for the so called $E - b_1 - b_2$ -problem [5] form diagonal in S and M_S

$$\begin{pmatrix} V_{b_{1g}}^\tau Q_{b_{1g}}^\tau & V_{b_{2g}}^\tau Q_{b_{2g}}^\tau \\ V_{b_{2g}}^\tau Q_{b_{2g}}^\tau & -V_{b_{1g}}^\tau Q_{b_{1g}}^\tau \end{pmatrix}, \quad \tau = {}^1E_u, {}^3E_u. \quad (3)$$

The singlet terms 1E_u and ${}^1A_{1g}$ interact due to linear vibronic coupling

$$\langle 00A_{1g}|V_{vib}|00E_u^i\rangle = \sum_{e_u} V_e Q_{e_u^i} \quad (4)$$

determined by active vibrational coordinates $Q_{e_u^x}, Q_{e_u^y}$. For the CuO_4 cluster there are three normal coordinates with e_u -symmetry, however, below we restrict ourselves with the choice of the one active e_u -vibration with an appropriate linear vibronic coupling constant V_e .

The sum of electronic Hamiltonian \hat{V}_{el} , elastic energy \hat{V}_Q , and vibronic Hamiltonian \hat{V}_{vib} for the singlet $S = 0$ spin manifold ${}^1E_u, {}^1A_{1g}$ could be written as:

$$\hat{U}(Q) = \hat{V}_{el} + \hat{V}_Q + \hat{V}_{vib} = \sum_i \frac{\omega_i^2 Q_i^2}{2} \cdot \hat{I} + \begin{pmatrix} -\Delta + V_z Q_z & V_e Q_x & V_e Q_y \\ V_e Q_x & V_\alpha Q_\alpha & V_\beta Q_\beta \\ V_e Q_y & V_\beta Q_\beta & -V_\alpha Q_\alpha \end{pmatrix}, \quad (5)$$

where the indices both for the coupling coefficient and normal coordinates are defined as follows: $a_{1g} \rightarrow z$, $e_u^x \rightarrow x$, $e_u^y \rightarrow y$, $b_{1g} \rightarrow \alpha$, $b_{2g} \rightarrow \beta$.

An important information for the PJT center could be obtained with examination of the adiabatic potential (AP) sheets $\varepsilon(Q)$, which are roots of the characteristic equation for $\hat{U}(Q)$. In our case this is reduced to a cubic equation with an extremely complicated expression for the roots. The coordinates of the minima Q^0 , energy and structure of electronic wave function at Q^0 and curvature of energy sheet near Q^0 can be obtained by the Opik-Pryce method [6]. An eigenvalue problem is treated in framework of this method only for extremal points of the AP with taking account of the relation between the extremum coordinates and the wave function in Q^0 which follows from the Hellmann-Feynman theorem:

$$\frac{\partial \varepsilon}{\partial Q} = \frac{\partial}{\partial Q} \langle \psi | \hat{U}(Q) | \psi \rangle = \left\langle \psi \left| \frac{\partial \hat{U}(Q)}{\partial Q} \right| \psi \right\rangle. \quad (6)$$

It should be noted that the Opik-Pryce method does not permit to find special points of the AP without definite values of the derivative, however namely such a situation occurs for the upper sheets of the AP. The type of minima can be derived from the curvature analysis for $\varepsilon(Q)$ near Q^0 . The $\varepsilon(Q)$ is found as the second-order correction to $\varepsilon(Q^0)$:

$$\varepsilon_-(Q) \approx \varepsilon_-(Q^0) + \langle \psi | \hat{U}_2(Q) | \psi \rangle + \sum_i' \frac{|\langle \psi_i | \hat{U}_1(Q) | \psi \rangle|^2}{\varepsilon_-(Q^0) - \varepsilon_i(Q^0)} \quad (7)$$

$$\hat{U}_1(Q) = \sum_i \frac{\partial \hat{U}(Q^0)}{\partial Q_i} q_i, \quad \hat{U}_2(Q) = \frac{1}{2} \sum_{ij} \frac{\partial^2 \hat{U}(Q^0)}{\partial Q_i \partial Q_j} q_i q_j, \quad q_i = Q_i - Q_i^0,$$

where $|\psi_i\rangle$ and $\varepsilon_i(Q^0)$ are eigenfunctions and eigenvalues of $\hat{U}(Q^0)$, and the prime at sum mark indicates the singular term is omitted.

The relations between the extremum coordinates for the AP and the wave function coefficients are

$$\begin{aligned} Q_z^0 &= -q_z^{(0)}z^2, & Q_x^0 &= -2q_x^{(0)}zx, & Q_y^0 &= -2q_y^{(0)}zy, \\ Q_\alpha^0 &= -q_\alpha^{(0)}(x^2 - y^2), & Q_\beta^0 &= -2q_\beta^{(0)}xy, \end{aligned} \quad (8)$$

where $q_i^{(0)} = V_i/\omega_i^2$ and we have denoted the coefficients of decomposition of the electronic wave function as z , x and y for $|00A_{1g}\rangle$, $|00E_u^x\rangle$ and $|00E_u^y\rangle$ respectively. The eigenvalue problem for V_{vib} in the exrtremum points of the AP is given by:

$$\begin{pmatrix} -\Delta - 2E_{JT}^z z^2 & -4E_{JT}^e zx & -4E_{JT}^e zy \\ -4E_{JT}^e zx & -2E_{JT}^\alpha (x^2 - y^2) & -4E_{JT}^\beta xy \\ -4E_{JT}^e zy & -4E_{JT}^\beta xy & 2E_{JT}^\alpha (x^2 - y^2) \end{pmatrix} \begin{pmatrix} z \\ x \\ y \end{pmatrix} = \lambda \begin{pmatrix} z \\ x \\ y \end{pmatrix}, \quad (9)$$

where $E_{JT}^i = \frac{1}{2}V_i q_i^{(0)} = V_i^2/2\omega_i^2$ is the specific JT-energy. The system (9) supplemented with a normalization condition $x^2 + y^2 + z^2 = 1$ has 13 solutions, which are listed in the Table 1. An expressions for the corresponding quadratic form of the AP-sheet near extreme point are given in the Table 2. These solutions could be divided into three groups.

1. The first group NJT (non-JT) contains one solution. Electronic part of the wave function in the exrtemal point is pure $|00A_{1g}\rangle$. The NJT-extremum is the minimum on the lower sheet of AP if $b < 0$ ($b = -\Delta + 4E_{JT}^e - 2E_{JT}^z$) and this is the minimum on the upper sheet of AP if $\Delta + 2E_{JT}^z < 0$. In both cases the weak pseudo-Jahn-Teller effect takes place, when due to weakness of vibronic interaction in comparison with initial splitting of electronic levels Δ there are no low symmetry distortions of the CuO_4 cluster. Due to vibronic interaction it occurs a renormalization of the local e_u -vibration frequency:

$$\left(\tilde{\omega}_e^{(NJT)}\right)^2 = \omega_e^2(1 - \eta_z), \quad \eta_z = \frac{4E_{JT}^e}{\Delta + 2E_{JT}^z}. \quad (10)$$

2. The second group JT_i ($i = \alpha, \beta$) contains four solutions. These are similar to the results of the well known $E - b_1 - b_2$ -problem. The wave function at the extremum points is a pure E_u -superposition. In further analysis the rhombic mode with larger JT-energy will be called the "strong" (σ) mode, and the rhombic mode with smaller JT-energy will be called the "weak" (σ') one: $E_{JT}^\sigma > E_{JT}^{\sigma'}$, ($\sigma, \sigma' = \alpha, \beta$); for the $E - b_1 - b_2$ -problem the E_{JT}^σ is the Jahn-Teller stabilization energy. From four exrtremum points only the JT_σ pair will be minima. The minima are located on the lower sheet of the AP if $a_\sigma < 0$ ($a_\sigma = \Delta + 4E_{JT}^e - 2E_{JT}^\sigma$), and on the middle one if $\Delta - 2E_{JT}^\sigma > 0$. The $JT_{\sigma'}$

pair represent saddle points. The wave functions at the minima are orthogonal each other. If $E_{JT}^\sigma = E_{JT}^{\sigma'}$ the equipotential continuum of minima exists. The frequency of the σ -mode does not change, and frequency of σ' -mode is renormalized due to vibronic interaction:

$$\tilde{\omega}_\sigma^2 = \omega_\sigma^2, \quad \tilde{\omega}_{\sigma'}^2 = \omega_{\sigma'}^2 (1 - \lambda_\sigma), \quad \lambda_\sigma = \frac{E_{JT}^{\sigma'}}{E_{JT}^\sigma}. \quad (11)$$

It should be noted here that a type (B_{1g} or B_{2g}) of the ground JT-mode is of principal importance for the physics of the copper oxides. This is determined by the competition of the vibronic parameters for the $Cu3d-O2p$ - and $O2p-O2p$ -bonds minimizing the B_{1g} - and B_{2g} -modes, respectively.

For the e_u -vibrations the JT_i solutions correspond to the weak pseudo-Jahn-Teller effect: only renormalization of the local e_u -vibration occurs. If α -mode is strong, then the minimum coordinates determine the rhombic distortion of the CuO_4 cluster along x - or y -direction (Fig.3). Accordingly, the softening of the e_u^x - or e_u^y -vibration occurs; but as both minima are equivalent, the frequencies of the local e_u -modes remain twice degenerate. In a case of "strong" β -mode with rectangular distortion of the CuO_4 cluster, the softening of that e -mode occurs, which co-directs to the cluster distortion. In all cases the expression for the renormalized local e_u -mode frequency is written as:

$$\left(\tilde{\omega}_e^{(JT)}\right)^2 = \omega_e^2 (1 - \kappa_\sigma), \quad \kappa_\sigma = \frac{4E_{JT}^\sigma}{-\Delta + 2E_{JT}^\sigma}. \quad (12)$$

3. The third group PJT_i ($i = \alpha, \beta$) includes eight solutions and corresponds to the most complicated case of the strong pseudo-Jahn-Teller effect. In this case the wave functions at the extremum points are the $A_{1g} - E_u$ -hybrid states. The coefficients of the appropriate linear combination depend on the initial splitting Δ and the JT-energies. The four from the eight PJT_σ -extrema (σ - the "strong" rhombic mode) are the minima if $a_\sigma > 0$ and $b > 0$. All the PJT_σ -minima are equivalent and allocated on the lower sheet of the AP. An arrangement of the minima in a space of the normal coordinates of the CuO_4 cluster is schematically shown in Fig.4. The wave functions at the minima are not orthogonal each other, that is a characteristic feature of the strong pseudo-Jahn-Teller effect. The four $PJT_{\sigma'}$ -extrema (σ' - the "weak" rhombic mode) are saddle points. A specific case of degeneracy for the JT-energies of rhombic modes should be investigated separately.

The rhombic distortion of the CuO_4 cluster at the minimum points with the nonzero plane quadrupole moment is accompanied by the co-directed e_u -distortion with the electric dipole moment. The possible PJT_σ distortions are shown in Fig.3.

Close to minimum M the equipotential surface of the quadratic form $\varepsilon(Q - Q^{(0,M)})$ is a five-dimensional ellipsoid with the center located at $Q^{(0,M)}$ and principal axes to be turned with regard to basic ones. The σ -mode at minimum

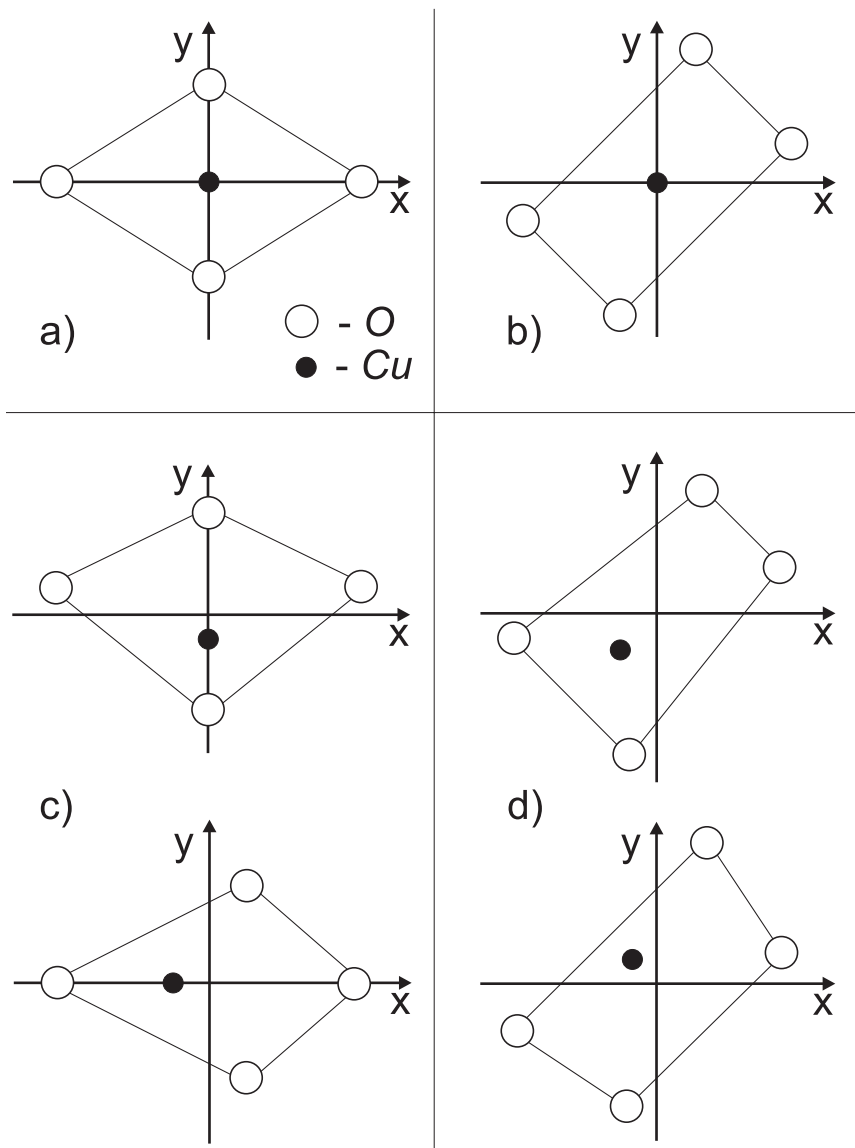


Figure 3: Possible distortions of the CuO_4 -cluster in the a) JT_α -minimum; b) JT_β -minimum; c) PJT_α -minimum (the dipole moment is oriented along the CuO_4 -cluster diagonal); b) PJT_β -minimum (the rotation angle value for the dipole moment with respect to that in PJT_α -minima is $\phi = \pi/4$).

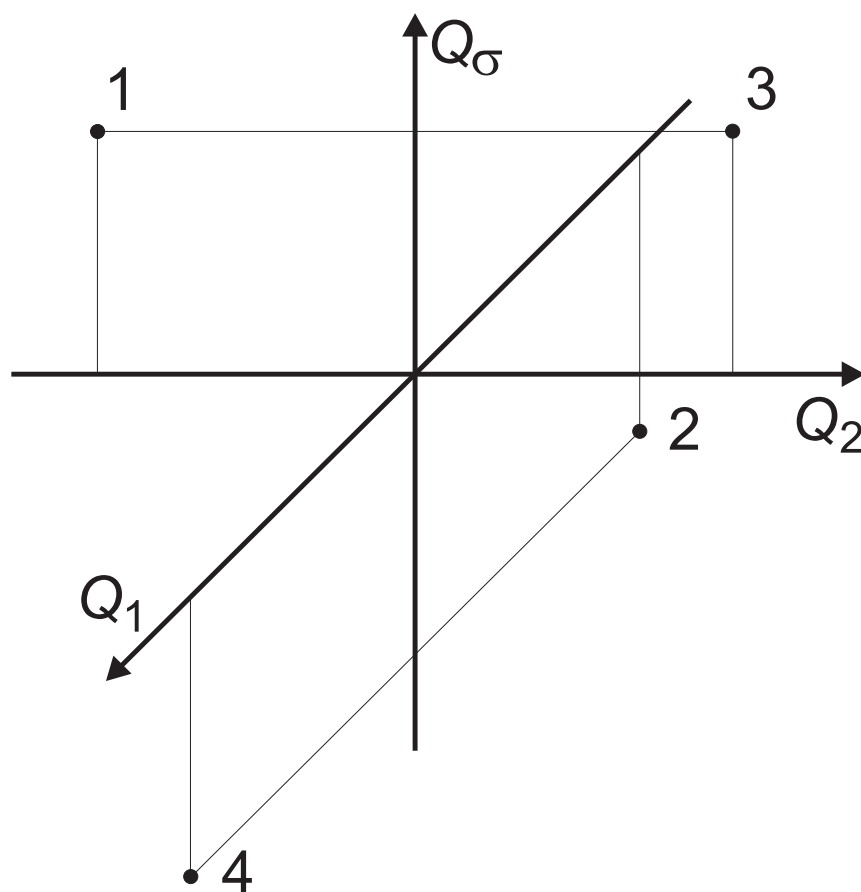


Figure 4: The allocation of the PJT_σ -minima in a space of symmetric coordinates Q_σ, Q_1, Q_2 (σ is the "strong" rhombic mode). If $\sigma = \alpha$, then $Q_1 = Q_x$, $Q_2 = Q_y$; if $\sigma = \beta$, then $Q_1 = \frac{Q_x + Q_y}{2}$, $Q_2 = \frac{-Q_x + Q_y}{2}$.

is mixed with co-directed e_u -mode and a_{1g} -mode giving rise to three local hybrid modes. The σ' -mode is mixed with the second e_u -mode giving rise to two local hybrid modes. The mixing coefficients are proportional to the appropriate vibronic coupling constants.

In case $V_z = 0$ the frequencies of the normal local hybrid modes are written as:

$$(Q_{\sigma'}, \tilde{Q}_1) : \quad \omega_{\pm}^2 = \frac{A+B}{2} \pm \sqrt{\left(\frac{A-B}{2}\right)^2 + C^2}, \quad (13)$$

where

$$A = \omega_e^2 (1 - \nu_\sigma^2), \quad B = \omega_{\sigma'}^2 (1 - \rho_\sigma^2), \quad C = \omega_e \omega_{\sigma'} \nu_\sigma \rho_\sigma,$$

$$\nu_\sigma = \sqrt{\frac{E_{JT}^e a_\sigma}{E_{JT}^e a_\sigma + E_{JT}^\sigma b}}, \quad \rho_\sigma = \sqrt{\frac{E_{JT}^{\sigma'} b}{E_{JT}^e a_\sigma + E_{JT}^\sigma b}},$$

and

$$(Q_\sigma, \tilde{Q}_2) : \quad \omega'_{\pm}{}^2 = \frac{D+E}{2} \pm \sqrt{\left(\frac{D-E}{2}\right)^2 + F^2}, \quad (14)$$

where

$$D = \omega_e^2 (1 - \nu_\sigma^2), \quad B = \omega_{\sigma'}^2 (1 - \mu_\sigma^2), \quad F = \omega_e \omega_{\sigma'} \nu_\sigma \mu_\sigma,$$

$$\mu_\sigma = \sqrt{\frac{E_{JT}^\sigma a_\sigma b}{E_{JT}^e (a_\sigma + b)^2}}, \quad \nu_\sigma = \frac{a_\sigma - b}{a_\sigma + b}.$$

For minima 1 and 3 $\tilde{Q}_1 = Q_x$ if $\sigma = \alpha$ (Q_1 if $\sigma = \beta$), $\tilde{Q}_2 = Q_y$ if $\sigma = \alpha$ (Q_2 if $\sigma = \beta$); for minima 2 and 4 $\tilde{Q}_1 = Q_y$ if $\sigma = \alpha$ (Q_2 if $\sigma = \beta$), $\tilde{Q}_2 = Q_x$ if $\sigma = \alpha$ (Q_1 if $\sigma = \beta$). Due to equivalence of minima all local frequencies coincide.

Conditions for the emergence of the certain type minima on the lower sheet of the AP will be determined mainly by the following quantities:

$$a_\sigma = \Delta + 4E_{JT}^e - 2E_{JT}^\sigma, \quad b = -\Delta + 4E_{JT}^e - 2E_{JT}^\sigma. \quad (15)$$

The type of minima on the lower sheet of the AP for various combinations of signs for the a_σ and b is shown in Table 3. The diagram of states of the lower sheet of the AP in a space of parameters Δ , E_{JT}^σ and E_{JT}^e at constant value of $E_{JT}^{z,0}$ is shown in Fig.5. A cross-section of the parameter space for a constant value of E_{JT}^e is shown in Fig.6. If $\Delta > 0$ the lowest ${}^1A_{1g}$ level is well isolated and the corresponding lower sheet of the AP has a rather trivial NJT minimum. In contrast, at $\Delta < 0$ the 1E_u term becomes the lower and an usual $E - b_1 - b_2$ -problem with two JT_σ minima on the lower sheet of the AP occurs. With coming together the ${}^1A_{1g}$ and 1E_u terms are mixed by e_u -mode and e_u -frequency is renormalized. An appropriate process depending on magnitude of E_{JT}^σ is accompanied by a formation of four PJT $_\sigma$ -minima or three

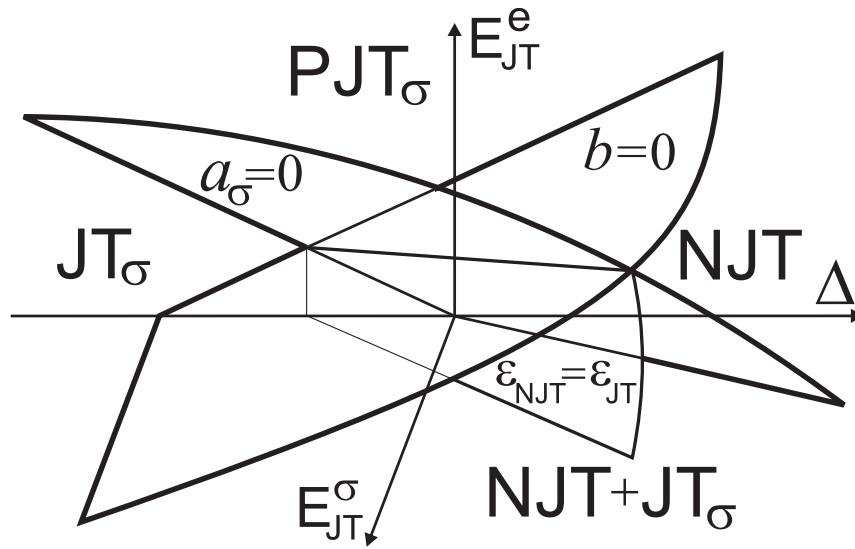


Figure 5: The diagram of the lower AP sheet states in the $(\Delta, E_{JT}^\sigma, E_{JT}^e)$ -space at certain fixed $E_{JT}^z = E_{JT}^{z,0}$ value. The planes $a_\sigma = 0$ and $b = 0$ divide the $(\Delta, E_{JT}^\sigma, E_{JT}^e)$ -space into four parts corresponding to NJT -, JT_σ -, PJT_σ - or $NJT + JT_\sigma$ -type of the lower AP sheet minima. In the $NJT + JT_\sigma$ region the plane is shown, where the NJT - and JT_σ -minimum energies are equal.

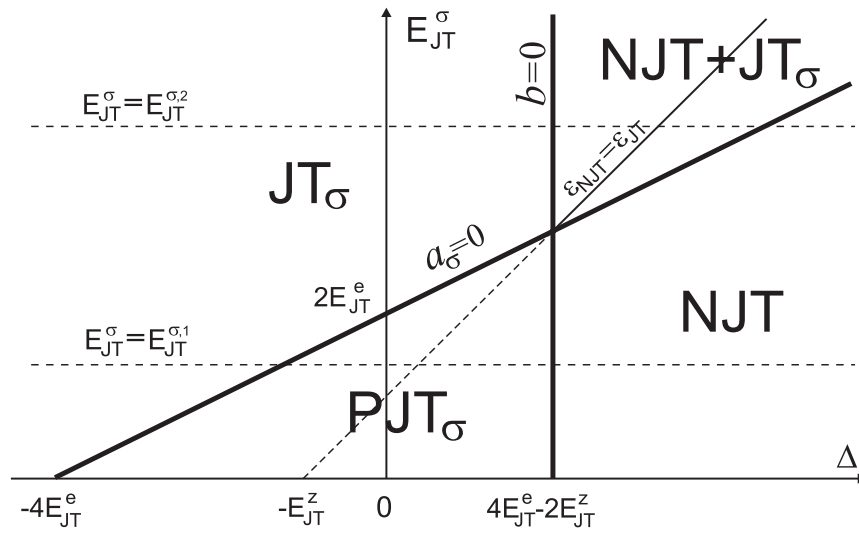


Figure 6: The diagram of states of the lower AP-sheet on the (Δ, E_{JT}^σ) -plane at certain fixed E_{JT}^z and E_{JT}^e value. The boundaries $a_\sigma = 0$ and $b = 0$ of the regions with different type of the lower AP-sheet minima are shown. The lines $E_{JT}^\sigma = E_{JT}^{\sigma,1}$ and $E_{JT}^\sigma = E_{JT}^{\sigma,2}$ correspond to the two different relative intensities of vibronic coupling via σ -mode and e_u -mode.

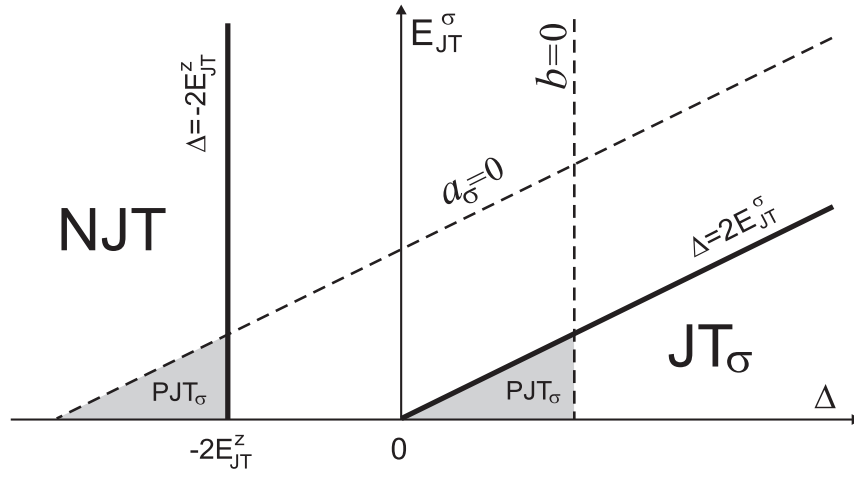


Figure 7: The diagram of states of the upper AP sheets on the (Δ, E_{JT}^σ) -plane at certain fixed E_{JT}^z and E_{JT}^e value. In region to the left of the $\Delta = -2E_{JT}^z$ line there is NJT -minimum on the upper AP-sheet and only the trivial non-analytical minimum on the middle AP-sheet. In the region to the right of the $\Delta = 2E_{JT}^\sigma$ line there is JT_σ -minima on the middle AP-sheet and the trivial non-analytical minimum on the upper AP-sheet. At $E_{JT}^z < 2E_{JT}^e$ the regions of parameters exist where the PJT_σ -minima on the lower AP-sheet coexist with the NJT -minimum on the upper sheet or with the JT_σ -minima on the middle sheet. Between the $\Delta = -2E_{JT}^z$ and $\Delta = 2E_{JT}^\sigma$ lines only the trivial non-analytical minima on the upper sheets exist.

(NJT+JT $_{\sigma}$)-minima. These two possibilities correspond to lines $E_{JT}^{\sigma} = E_{JT}^{\sigma,1}$ and $E_{JT}^{\sigma} = E_{JT}^{\sigma,2}$ in Fig.7.

With a motion along line $E_{JT}^{\sigma} = E_{JT}^{\sigma,1}$ from $-\infty$ up to $+\infty$ the curvature of the JT $_{\sigma}$ -minima along e_u -directions decreases up to zero on a line $a_{\sigma} = 0$. In this point the JT $_{\sigma}$ -minima transform into saddle points with simultaneous appearance of the PJT $_{\sigma}$ -minima (one of the JT $_{\sigma}$ -minima splits along Q_1 -, another one splits along Q_2 -direction). From the line $a_{\sigma} = 0$ up to $b = 0$ the magnitude of rhombic distortion decreases up to zero on a line $b = 0$. The magnitude of e_u -coordinates of minima firstly increases, then decreases up to zero, reaching a maximum on line $\Delta = -E_{JT}^{\sigma} + E_{JT}^z$. The Q_z -coordinate increases linearly ($\sim a_{\sigma}$) from zero up to $-q_z^{(0)}$ on a line $b = 0$. Thus, the four PJT $_{\sigma}$ -minima transform into one NJT-minimum. Further, with $\Delta \rightarrow +\infty$ the A_{1g} and E_u terms interact weaker and $\tilde{\omega}_e \rightarrow \omega_e$.

The situation with emergence of the PJT $_{\sigma}$ -minima is realized when the e_u -mode driven interaction of the A_{1g} and E_u terms is rather effective. When $E_{JT}^{\sigma} > 4E_{JT}^e - E_{JT}^z$ (for example $E_{JT}^{\sigma} = E_{JT}^{\sigma,2}$), the σ -mode driven interaction becomes more effective. In this case at $b = 0$ the NJT minimum appears on the lower sheet of the AP together with JT $_{\sigma}$ -minima. All three minima have the same energy on the line $\Delta = -E_{JT}^{\sigma} + E_{JT}^z$. Further, at $\Delta \rightarrow +\infty$ JT $_{\sigma}$ -minima become more flat, without varying their coordinates, and at $a_{\sigma} = 0$ only the NJT-minimum remains.

In Fig.8 the diagram of the upper sheets of the AP is shown.

4 Vibronic states in a presence of the spin-orbit coupling.

Without taking account of the spin-orbit coupling the 3E_u term is isolated, and it has the six-times degenerated ground vibronic state. The spin-orbit coupling mixes the $M_S = 0$ states of the 3E_u and 1E_u terms. As well, this coupling splits lower vibronic states of the 3E_u term which have $M_S = \pm 1$.

4.1 The $M_S = 0$ states.

4.1.1 The well isolated ${}^1A_{1g}$ term.

If the ${}^1A_{1g}$ and ${}^1,{}^3E_u$ terms are well separated in energy ($\Delta_{AE} \gg \Delta_E, \lambda$) it is possible to consider the AP within a basis of the $|00E_u^x\rangle, |00E_u^y\rangle, |10E_u^x\rangle, |10E_u^y\rangle$ states, and then take into account vibronic coupling with the of ${}^1A_{1g}$ term as

perturbation. The potential energy matrix has a form:

$$\hat{U}(Q) = \sum_i \frac{\omega_i^2 Q_i^2}{2} \cdot \hat{I} + \begin{pmatrix} -\Delta_E + V_\alpha Q_\alpha & V_\beta Q_\beta & 0 & -i\lambda \\ V_\beta Q_\beta & -\Delta_E - V_\alpha Q_\alpha & i\lambda & 0 \\ 0 & -i\lambda & \Delta_E + V_\alpha Q_\alpha & V_\beta Q_\beta \\ i\lambda & 0 & V_\beta Q_\beta & \Delta_E - V_\alpha Q_\alpha \end{pmatrix}, \quad (16)$$

where λ is a submatrix element of the spin-orbit coupling. The eigenvalues and eigenvectors of $\hat{U}(Q)$ are written as

$$\begin{aligned} \varepsilon_1 &= \Sigma - \sqrt{(\Delta_E + \rho)^2 + \lambda^2} & |1\rangle &= -i \sin \eta_1 |-\rho, 0\rangle + \cos \eta_1 |\rho, 1\rangle, \\ \varepsilon_2 &= \Sigma - \sqrt{(\Delta_E - \rho)^2 + \lambda^2} & |2\rangle &= i \sin \eta_2 |\rho, 0\rangle + \cos \eta_2 |-\rho, 1\rangle, \\ \varepsilon_3 &= \Sigma + \sqrt{(\Delta_E - \rho)^2 + \lambda^2} & |3\rangle &= \cos \eta_2 |\rho, 0\rangle + i \sin \eta_2 |-\rho, 1\rangle, \\ \varepsilon_4 &= \Sigma + \sqrt{(\Delta_E + \rho)^2 + \lambda^2} & |4\rangle &= \cos \eta_1 |-\rho, 0\rangle - i \sin \eta_1 |\rho, 1\rangle, \end{aligned} \quad (17)$$

where

$$\Sigma = \sum_i \frac{\omega_i^2 Q_i^2}{2}, \quad \rho = \sqrt{(V_\alpha Q_\alpha)^2 + (V_\beta Q_\beta)^2},$$

$$|\rho, S\rangle = \cos \theta |S0E_u^x\rangle + \sin \theta |S0E_u^y\rangle, \quad |-\rho, S\rangle = -\sin \theta |S0E_u^x\rangle + \cos \theta |S0E_u^y\rangle,$$

$$\tan 2\theta = \frac{V_\beta Q_\beta}{V_\alpha Q_\alpha}, \quad \tan 2\eta_1 = \frac{\lambda}{-\Delta_E - \rho}, \quad \tan 2\eta_2 = \frac{\lambda}{-\Delta_E + \rho}.$$

The minima of the lower sheet of the AP are located on Q_σ -axis (with $E_{JT}^\sigma > E_{JT}^{\sigma'}$, $\sigma, \sigma' = \alpha, \beta$) in points, which represent solutions of the equation:

$$\frac{|Q_\sigma|}{q_\sigma^{(0)}} = \left(1 + \frac{\lambda^2}{(V_\sigma |Q_\sigma| + \Delta_E)^2} \right)^{-\frac{1}{2}}. \quad (18)$$

The $Q_{\Gamma\gamma} = 0$ is a point of discontinuity of the derivative. The non-trivial minima, which correspond to the low-symmetric distortions of the cluster, exist for the arbitrary large λ , but with $\lambda \rightarrow \infty$ the minima depth and the distortions magnitude become negligibly small.

A ground vibronic state is twice degenerated. In the strong coupling scheme it is realized due to orthogonality of electronic states belonging to different minima of the AP. In a case $\lambda \ll E_{JT}^\sigma$ the expressions for the minimum points and their energy are written as:

$$Q_\sigma = \pm \tilde{q}_\sigma^{(0)}, \quad \tilde{q}_\sigma^{(0)} = q_\sigma^{(0)} \left(1 - \frac{\lambda^2}{2(\Delta_E + 2E_{JT}^\sigma)^2} \right), \quad (19)$$

$$\varepsilon_0 = -\Delta_E - E_{JT}^\sigma - \frac{\lambda^2}{2(\Delta_E + 2E_{JT}^\sigma)} .$$

The mixing coefficient for the triplet spin states with the ${}^1A_{1g}$ term wave function is proportional to

$$\frac{\lambda}{\Delta_E + \Delta_{AE} + E_{JT}^\sigma} . \quad (20)$$

4.1.2 The strong PJT-effect for the singlet spin states.

In this case it is necessary to consider a mixing of the tunnel states with lower vibronic states of 3E_u term due to the spin-orbit coupling. The only non-zero matrix elements are those between the tunnel E_u -states and the lower vibronic states of 3E_u term with $M_S = 0$. The effective Hamiltonian matrix is

$$\begin{pmatrix} -\Delta'_E & 0 & 0 & -i\lambda' \\ 0 & -\Delta'_E & i\lambda' & 0 \\ 0 & -i\lambda' & \Delta'_E & 0 \\ i\lambda' & 0 & 0 & \Delta'_E \end{pmatrix}, \quad (21)$$

where $2\Delta'$ is an appropriate energy splitting, λ' is a modified matrix element of the spin-orbit coupling:

$$\lambda' = \lambda N_{E_u}^{-1} \sqrt{2} d_\sigma \langle \chi_M^{(\sigma)} | \tilde{\chi}_0^{(\sigma)} \rangle, \quad (22)$$

where $\chi_M^{(\sigma)}$ and $\tilde{\chi}_0^{(\sigma)}$ are the ground state vibrational functions, which are centered in the minimum M of PJT $_\sigma$ -type and in the minimum of the AP of the $E - b_1 - b_2$ -problem with opposite to M sign of σ -mode, respectively.

4.1.3 The singlet-triplet asymmetry of the vibronic coupling.

Let the difference in the linear vibronic coupling constants for singlet 1E_u and 3E_u triplet states corresponds to the following inequalities for the JT-energies: $E_{JT}^\alpha({}^1E_u) > E_{JT}^\beta({}^3E_u)$ and $E_{JT}^\alpha({}^1E_u) < E_{JT}^\beta({}^3E_u)$.

The minima of the AP of the 1E_u term are located on the Q_α -axis, and those of the E_u term are located on the Q_β -axis. If the sheets of the AP for different terms intersect, taking account of the spin-orbit coupling could result in a complicated form of the AP with four minima. The states in minima located on the same axis are orthogonal to each other, and those located on different axis are not. Hence, even if $\Delta_E = 0$ the lower vibronic states are two doublets, which are separated by the tunnel splitting $\tilde{\Delta}$. The frequency related to $\tilde{\Delta}$ corresponds to the combined pulsing motion of the electronic and nuclear density between b_{1g} - and b_{2g} -distortions of CuO_4 -cluster.

4.2 The $M_S = \pm 1$ states.

A joint operation of the vibronic and spin-orbital coupling for the $M_S = \pm 1$ states within the 3E_u manifold is described by the matrix

$$V_\alpha Q_\alpha \tilde{\sigma}_z + V_\beta Q_\beta \tilde{\sigma}_x + iM_S \lambda_1 \tilde{\sigma}_y, \quad (23)$$

where λ_1 is a submatrix element for the spin-orbital coupling within the orbital part of the 3E_u manifold, $\tilde{\sigma}_i$ are the Pauli matrices, and the energy is counted off the 3E_u manifold.

The lower sheet of the adiabatic potential has four extrema at points

$$q_i^{(0,\pm)} = \pm l_i \sqrt{2\tilde{E}_{JT}^i (1 - p_i^2)}, \quad i = \alpha, \beta, \quad (24)$$

where $l_i = \sqrt{\hbar/\omega_i}$, $\tilde{E}_{JT}^i = E_{JT}^i/\hbar\omega_i$, $p_i = \lambda_1/2E_{JT}^i$, and $q_i^{(0,\pm)} = 0$ at $|p_i| \geq 1$. The parameter p_i equals to the ratio of the E_u -level splitting due to the spin-orbital coupling ($2\lambda_1$) to that of due to the vibronic coupling ($4E_{JT}^i$). At $|p_i| \geq 1$ ($i = \alpha, \beta$) we come to the weak pseudo-Jahn-Teller effect with the only minimum at $q_i^{(0,\pm)} = 0$ ($i = \alpha, \beta$) and with the effective local vibration frequencies

$$\tilde{\omega}_i^2 = \omega_i^2 (1 - |p_i|^{-1}). \quad (25)$$

At $|p_i| \leq 1$ ($E_{JT}^\sigma > E_{JT}^{\sigma'}$) the strong pseudo-Jahn-Teller effect occurs with the AP-minima at $q_\sigma^{(0,\pm)}$, and with the AP-saddle points at $q_{\sigma'}^{(0,\pm)}$. The effective frequencies for the local vibrations at the AP-minima and corresponding energies are derived as follows:

$$\begin{aligned} \tilde{\omega}_\sigma^2 &= \omega_\sigma^2 (1 - p_\sigma^2), \\ \tilde{\omega}_{\sigma'}^2 &= \omega_{\sigma'}^2 (1 - \lambda_\sigma), \quad \lambda_\sigma = \frac{E_{JT}^{\sigma'}}{E_{JT}^\sigma}, \\ \varepsilon_- (q_\sigma^{(0,\pm)}) &= -E_{JT}^\sigma - \hbar\omega_\sigma p_\sigma. \end{aligned} \quad (26)$$

As is seen, unlike the usual $E - b_1 - b_2$ -problem, the σ -mode frequency is renormalized due to the spin-orbital coupling.

The electronic wave functions $\varphi_\pm^{(M_S)}$ in the $q_\sigma^{(0,\pm)}$ minima are reduced to the following form:

$$\begin{aligned} \varphi_+^{(M_S)} &= \frac{1}{\sqrt{2}} \left(i M_S \sqrt{1 - \sqrt{1 - p_\sigma^2}} |E_u^{(1)}\rangle + \sqrt{1 + \sqrt{1 - p_\sigma^2}} |E_u^{(2)}\rangle \right), \\ \varphi_-^{(M_S)} &= \frac{1}{\sqrt{2}} \left(\sqrt{1 + \sqrt{1 - p_\sigma^2}} |E_u^{(1)}\rangle + i M_S \sqrt{1 - \sqrt{1 - p_\sigma^2}} |E_u^{(2)}\rangle \right). \end{aligned} \quad (27)$$

In contrast to the above considered $E - b_1 - b_2$ -problem, taking account of the spin-orbital coupling results in the non-orthogonality of the wave functions for the minima of the lower sheet of the adiabatic potential:

$$\langle \varphi_+^{(M_S)} | \varphi_-^{(M_S)} \rangle = -i M_S p_\sigma \quad (28)$$

that leads to the tunnel splitting.

Varying the energy functional with the basis functions

$$\Psi = a \varphi_+^{(M_S)} \chi_+ + b \varphi_-^{(M_S)} \chi_-, \quad (29)$$

where χ_{\pm} are the vibration functions centered at $q_{\sigma}^{(0,\pm)}$, results in a matrix equation:

$$\begin{pmatrix} H_{++} & H_{+-} \\ H_{+-}^* & H_{++} \end{pmatrix} \begin{pmatrix} c_1 \\ c_2 \end{pmatrix} = E \begin{pmatrix} 1 & S_{+-} \\ S_{+-}^* & 1 \end{pmatrix} \begin{pmatrix} c_1 \\ c_2 \end{pmatrix}, \quad (30)$$

where

$$\begin{aligned} S &= \langle \varphi_+^{(M_S)} \chi_+ | \varphi_-^{(M_S)} \chi_- \rangle = -i M_S p_{\sigma} e^{-2\tilde{E}_{JT}^{\sigma} (1-p_{\sigma}^2)^{\frac{3}{2}}}, \\ H_{++} &= \hbar\omega_{\sigma} \left[\frac{2-p_{\sigma}^2}{4\sqrt{1-p_{\sigma}^2}} - \tilde{E}_{JT}^{\sigma} (1+p_{\sigma}^2) \right] + \hbar\omega_{\sigma'} \frac{2-\lambda_{\sigma}}{4\sqrt{1-\lambda_{\sigma}}}, \\ H_{+-} &= (H_{++} - \hbar\omega_{\sigma} B) S, \quad B = \tilde{E}_{JT}^{\sigma} (1-p_{\sigma}^2) (2-p_{\sigma}^2). \end{aligned} \quad (31)$$

The tunnel level energies and tunnel splitting are determined as follows:

$$\begin{aligned} E_g &= H_{++} - \frac{\hbar\omega_{\sigma} B |S|}{1+|S|}, \quad E_u = H_{++} + \frac{\hbar\omega_{\sigma} B |S|}{1-|S|}, \\ \Delta_1 &= E_g - E_u = 2\hbar\omega_{\sigma} \frac{B|S|}{1-|S|^2}. \end{aligned} \quad (32)$$

and appropriate vibronic wave functions can be represented as:

$$\begin{aligned} \Psi_g^{(1)} &= \frac{1}{\sqrt{2(1+|S|)}} \left(\varphi_+^{(1)} \chi_+ + i\varphi_-^{(1)} \chi_- \right); \\ \Psi_u^{(1)} &= \frac{1}{\sqrt{2(1-|S|)}} \left(i\varphi_+^{(1)} \chi_+ + \varphi_-^{(1)} \chi_- \right); \\ \Psi_g^{(-1)} &= \frac{1}{\sqrt{2(1+|S|)}} \left(i\varphi_+^{(-1)} \chi_+ + \varphi_-^{(-1)} \chi_- \right); \\ \Psi_u^{(-1)} &= \frac{1}{\sqrt{2(1-|S|)}} \left(\varphi_+^{(-1)} \chi_+ + i\varphi_-^{(-1)} \chi_- \right). \end{aligned} \quad (33)$$

In the limit $|p_{\sigma}| \ll 1$ for the magnitude of the tunnel splitting one obtains:

$$\Delta_1 = 2\lambda_1 e^{-2\tilde{E}_{JT}^{\sigma}}, \quad (34)$$

that might be interpreted as a result of the vibronic reduction for the purely spin orbital splitting.

5 Spin Hamiltonian of the PJT center.

A detailed pattern of the energy spectrum in the external magnetic field and the magneto-resonance properties of the PJT-centers are substantially depend

on the bare $A - E$ -splitting Δ , vibronic parameters and relative magnitude of the vibronic and spin-orbital coupling.

However, some common features are determined only by the symmetry considerations, in particular, by the C_4 axial symmetry and the specific properties of the bare electronic basis functions. So, the orbital doublet 1,3E_u terms are characterized by the nonquenched highly anisotropic (Izing like) orbital moment $\tilde{l} = 1/2$ oriented only along the C_4 axis.

Without account of vibronic coupling the effective spin Hamiltonian for the 1,3E_u terms could be represented as follows:

$$H = \lambda_1 \tilde{l}_z \hat{S}_z + \beta H_z g_l \tilde{l}_z \hat{I} + 2\beta \sum_{i=x,y,z} H_i \hat{S}_i, \quad (35)$$

where β is the Bohr magneton, \hat{S}_i are spin matrices ($S = 0$ for the spin singlet 1E_u term), g_l is effective orbital g -factor for the 1,3E_u term, which value is determined by the structure of the electronic e_u -function. Here, the first term describes the spin-orbital coupling, the second and the third terms correspond to the orbital and spin Zeeman coupling, respectively, with the purely isotropic spin g -tensor: $g_x = g_y = g_z = 2$. Taking account of the spin-orbital 1E_u - 3E_u -mixing leads to an emergence of the spin anisotropy with an additive contribution to the effective spin Hamiltonian:

$$V_{an} = D \hat{S}_z^2, \quad D = \Delta_{st} - \sqrt{\Delta_{st}^2 + \lambda^2} \approx -\frac{\lambda^2}{2\Delta_{st}}, \quad (36)$$

and the effective axial anisotropy of the spin g -tensor: $g_z = 2$, $g_x = g_y = 2 \cos \theta$, where

$$\cos \theta = \frac{1}{\sqrt{2}} \sqrt{1 + \frac{\Delta_{st}}{\sqrt{\Delta_{st}^2 + \lambda^2}}} \approx 1 - \frac{\lambda^2}{8\Delta_{st}^2}. \quad (37)$$

Taking account of the vibronic coupling upon the conditions of the weak pseudo-Jahn-Teller effect ($p_\sigma = \lambda_1/2E_{JT}^g > 1$) does not vary a form of the effective spin Hamiltonian since the vibronic distortions are suppressed by the spin-orbital coupling. With the strong pseudo-Jahn-Teller effect ($p_\sigma = \lambda_1/2E_{JT}^g < 1$) one should make use of the vibronic states (33), that results in a very complicated spin-vibronic effective Hamiltonian. A relatively simple situation occurs at $p_\sigma^2 \ll 1$, and small values of the overlap for the oscillatory functions when neglecting the spin-orbital 1E_u - 3E_u -mixing, we come to effective Hamiltonian:

$$H = -\beta H_z g_1 \langle \chi_+ | \chi_- \rangle \tilde{l}_z \hat{I} - \beta \sum_{i=x,y,z} H_i g_{ij} \hat{S}_j, \quad (38)$$

where the overlap integral $\langle \chi_+ | \chi_- \rangle$ is determined according to (31) and for the axial g -tensor: $g_z = 2 - p_\sigma g_1$, $g_x = g_y = 2$. It should be noted the principal difference in the g -factor anisotropy with and without vibronic effects.

The doublet of the states with different (\pm) projections of the effective orbital moment corresponds to the functions $\{\Psi_g^{(1)}, \Psi_g^{(0)}, \Psi_u^{(-1)}\}$ and $\{\Psi_u^{(1)}, \Psi_u^{(0)}, \Psi_g^{(-1)}\}$, respectively, where, along with the above defined functions (33), we have introduced

$$\begin{aligned}\Psi_g^{(0)} &= \frac{1}{\sqrt{2}} \left(\begin{array}{c} |E_u^{(2)}\rangle \chi_+^{(0)} + i |E_u^{(1)}\rangle \chi_-^{(0)} \\ |E_u^{(2)}\rangle \chi_+^{(0)} + |E_u^{(1)}\rangle \chi_-^{(0)} \end{array} \right), \\ \Psi_u^{(0)} &= \frac{1}{\sqrt{2}} \left(\begin{array}{c} |E_u^{(2)}\rangle \chi_+^{(0)} + i |E_u^{(1)}\rangle \chi_-^{(0)} \\ i |E_u^{(2)}\rangle \chi_+^{(0)} + |E_u^{(1)}\rangle \chi_-^{(0)} \end{array} \right).\end{aligned}\quad (39)$$

An upper label for the vibration function underlines the difference in the location of the minima for the $M_S = 0$ and $M_S \neq 0$ spin 3E_u -states within a lower sheet of the adiabatic potential. It should be noted also, that, in general, the overlap integral $\langle \chi_+ | \chi_- \rangle$ depends on the z -component of the magnetic field due to the orbital Zeeman coupling which contributes to the energy of the lower sheet of the adiabatic potential. At $\beta H_z \gg \lambda_1$ an expression for the corresponding energy acquires a form:

$$\varepsilon_- = \frac{1}{2} (\omega_\alpha^2 Q_\alpha^2 + \omega_\beta^2 Q_\beta^2) - \sqrt{(V_\alpha Q_\alpha)^2 + (V_\beta Q_\beta)^2 + (\beta H_z g_1)^2}. \quad (40)$$

6 Some experimental evidence of the singlet-triplet PJT-centers

Main hopes to the direct demonstration of the validity of the above model are connected with a reveal of the isolated PJT-center. In this connection let note the recent paper [7] which authors undertook the NQR-study of the hole centers CuO_4^{5-} in $La_2Cu_{0.5}Li_{0.5}O_4$. Their results can be interpreted as convincing evidence of the singlet-triplet PJT-structure of the hole center. This conclusion is based on the following:

1. The authors revealed the spin singlet ground state ($S = 0$) and the low lying spin triplet state ($S = 1$) with the singlet-triplet separation $\Delta_{st} = 0.13$ eV.
2. They observed anomalous weak temperature dependence of the relaxation rate at low temperatures that evidences the occurrence of the spinless multiplet structure in the CuO_4^{5-} -cluster ground state.
3. They revealed an appreciable spin contribution to the low temperature relaxation indicating the simultaneous occurrence of the ground state multiplet structure, the sufficiently low singlet-triplet separation and the intrinsic singlet-triplet spin-orbital mixing.
4. They observed the relaxation inequivalence of the various Cu sites quite natural for the PJT-centers in the conditions of the static JT-effect.

We think that the further investigations of this system can provide a valuable information about PJT-centers.

The Jahn-Teller hole centers like CuO_4^{5-} with the singlet-triplet quasi-degeneracy within ground state have been observed by ESR spectroscopy in

$LaSrAl_{1-x}Cu_xO_4$ which is isostructural to $La_{2-x}Sr_xCuO_4$ [8]. An important indication to the $O2p(\pi)$ nature of the doped holes and, consequently, to occurrence of the degeneracy for configurations like b_{1g}^2 and $b_{1g}e_u(\pi)$ was obtained by Yoshinari [9] after analysis of the ^{17}O Knight shift data in $YBa_2Cu_3O_{6+x}$.

Among diverse peculiarities of the spin-triplet PJT centers it should be especially emphasized a possible appearance of the so called "tunnel paramagnetic centers" [10] which spin states $S = 1, M_S = \pm 1$ and $S = 1, M_S = 0$, respectively, are localized within different wells of the adiabatic potential. In other words, different spin states correspond to different local distortions of the CuO_4 cluster. Spin dynamics and relaxation for the tunnel paramagnetic centers is crucially dependent on the magnitude and orientation of the external magnetic field. These centers could be relatively simply transferred to the metastable state.

It should be noted that we did not undertake the task of reviewing all the available experimental data confirming the PJT nature of the CuO_4 clusters in doped cuprates and comparing them with our model approach: it is a separate problem. At the same time, it should be noted that the PJT centers model is entirely based on the vast amount of the experimental material.

In conclusion, we would like to acknowledge the stimulating discussions with Prof. M.V.Eremin.

References

- [1] A.S.Moskvin, *JETP Lett.* **58**, 342 (1993)
- [2] A.S.Moskvin, N.N.Loshkareva, Yu.P.Sukhorukov, M.A.Sidorov, A.A.Samokhvalov, *JETP* **105**, 967 (1994).
- [3] A.S.Moskvin, *Physica C* **282-287**, 1807 (1997)
- [4] J.E. Hirsch, S. Tang, *Phys.Rev.* **B 40**, 2179 (1989)
- [5] I.B.Bersuker and V.Z.Polinger. *Vibronic Interactions in Molecules and Crystals* (Springer-Verlag, Berlin) 1989
- [6] U. Opik, M.H.L. Pryce. *Proc.Roy.Soc.* **A 238**, 425 (1957).
- [7] Y. Yoshinari, P.C. Hammel, J.A. Martindale, E. Moshopoulou, J.D. Thompson, *Phys. Rev. Lett.* **77**, 2069 (1996)
- [8] T.A.Ivanova, E.F.Kukovitsky, E.N.Nabiullin et al., *JETP Lett.* **57**, 64 (1993)
- [9] Y.Yoshinari, *Physica C* **276**, 147 (1997)
- [10] A.S. Moskvin, I.B. Krinetsky, R. Szymczak, Yu.D. Panov, S.V. Naumov, A.A. Samokhvalov, *Fizika Tverd. Tela* **39**, 474 (1997)

TABLES.

Table 1.

Type	N	$ 00A_{1g}\rangle$	$ 00E_u^x\rangle$	$ 00E_u^y\rangle$	Q_z^0	Q_α^0	Q_β^0	Q_x^0	Q_y^0
NJT	1	1	0	0	$-q_z^{(0)}$	0	0	0	0
JT_α	1	0	0	1	0	$q_\alpha^{(0)}$	0	0	0
	2	0	1	0	0	$-q_\alpha^{(0)}$	0	0	0
JT_β	1	0	$-1/\sqrt{2}$	$1/\sqrt{2}$	0	0	$q_\beta^{(0)}$	0	0
	2	0	$1/\sqrt{2}$	$1/\sqrt{2}$	0	0	$-q_\beta^{(0)}$	0	0
PJT_α	1	c_α	0	d_α	$-q_z^{(0)}c_\alpha^2$	$q_\alpha^{(0)}d_\alpha^2$	0	0	$-q_\epsilon^{(0)}2c_\alpha d_\alpha$
	2	c_α	d_α	0	$-q_z^{(0)}c_\alpha^2$	$-q_\alpha^{(0)}d_\alpha^2$	0	$-q_\epsilon^{(0)}2c_\alpha d_\alpha$	0
	3	c_α	0	$-d_\alpha$	$-q_z^{(0)}c_\alpha^2$	$q_\alpha^{(0)}d_\alpha^2$	0	0	$q_\epsilon^{(0)}2c_\alpha d_\alpha$
	4	c_α	$-d_\alpha$	0	$-q_z^{(0)}c_\alpha^2$	$-q_\alpha^{(0)}d_\alpha^2$	0	$q_\epsilon^{(0)}2c_\alpha d_\alpha$	0
PJT_β	1	c_β	$-d_\beta/\sqrt{2}$	$d_\beta/\sqrt{2}$	$-q_z^{(0)}c_\beta^2$	0	$q_\alpha^{(0)}d_\beta^2$	$q_\epsilon^{(0)}\sqrt{2}c_\beta d_\beta$	$-q_\epsilon^{(0)}\sqrt{2}c_\beta d_\beta$
	2	c_β	$d_\beta/\sqrt{2}$	$d_\beta/\sqrt{2}$	$-q_z^{(0)}c_\beta^2$	0	$-q_\alpha^{(0)}d_\beta^2$	$-q_\epsilon^{(0)}\sqrt{2}c_\beta d_\beta$	$-q_\epsilon^{(0)}\sqrt{2}c_\beta d_\beta$
	3	c_β	$d_\beta/\sqrt{2}$	$-d_\beta/\sqrt{2}$	$-q_z^{(0)}c_\beta^2$	0	$q_\alpha^{(0)}d_\beta^2$	$-q_\epsilon^{(0)}\sqrt{2}c_\beta d_\beta$	$q_\epsilon^{(0)}\sqrt{2}c_\beta d_\beta$
	4	c_β	$-d_\beta/\sqrt{2}$	$-d_\beta/\sqrt{2}$	$-q_z^{(0)}c_\beta^2$	0	$-q_\alpha^{(0)}d_\beta^2$	$q_\epsilon^{(0)}\sqrt{2}c_\beta d_\beta$	$q_\epsilon^{(0)}\sqrt{2}c_\beta d_\beta$

where

$$q_i^{(0)} = \frac{V_i}{\omega_i^2}, a_\sigma = \Delta + 4E_{JT}^e - 2E_{JT}^\sigma, b = -\Delta + 4E_{JT}^e - 2E_{JT}^z, c_\sigma = \sqrt{\frac{a_\sigma}{a_\sigma + b}}, d_\sigma = \sqrt{\frac{b}{a_\sigma + b}}.$$

Table 2.

Type	N	$2\varepsilon(q) - 2\varepsilon_0^\sigma - \sum_i \omega_i^2 q_i^2$
<i>NJT</i>	1	$-\omega_\varepsilon^2 \eta_z (q_x^2 + q_y^2)$
<i>JT$_\alpha$</i>	1	$-\omega_\varepsilon^2 \kappa_\alpha q_y^2 - \omega_\beta^2 \lambda_\alpha q_\beta^2$
	2	$-\omega_\varepsilon^2 \kappa_\alpha q_x^2 - \omega_\beta^2 \lambda_\alpha q_\beta^2$
<i>JT$_\beta$</i>	1	$-\omega_\varepsilon^2 \kappa_\beta q_2^2 - \omega_\alpha^2 \lambda_\beta q_\alpha^2$
	2	$-\omega_\varepsilon^2 \kappa_\beta q_1^2 - \omega_\alpha^2 \lambda_\beta q_\alpha^2$
<i>PJT$_\alpha$</i>	1	$-(\omega_\varepsilon \nu_\alpha q_x + \omega_\beta \rho_\alpha q_\beta)^2 - (\omega_z \tau_\alpha q_z + \omega_\alpha \mu_\alpha q_\alpha - \omega_\varepsilon \nu_\alpha q_y)^2$
	2	$-(\omega_\varepsilon \nu_\alpha q_y + \omega_\beta \rho_\alpha q_\beta)^2 - (\omega_z \tau_\alpha q_z - \omega_\alpha \mu_\alpha q_\alpha - \omega_\varepsilon \nu_\alpha q_x)^2$
	3	$-(\omega_\varepsilon \nu_\alpha q_x - \omega_\beta \rho_\alpha q_\beta)^2 - (\omega_z \tau_\alpha q_z + \omega_\alpha \mu_\alpha q_\alpha + \omega_\varepsilon \nu_\alpha q_y)^2$
	4	$-(\omega_\varepsilon \nu_\alpha q_y - \omega_\beta \rho_\alpha q_\beta)^2 - (\omega_z \tau_\alpha q_z - \omega_\alpha \mu_\alpha q_\alpha + \omega_\varepsilon \nu_\alpha q_x)^2$
<i>PJT$_\beta$</i>	1	$-(\omega_\varepsilon \nu_\beta q_1 - \omega_\alpha \rho_\beta q_\alpha)^2 - (\omega_z \tau_\beta q_z + \omega_\beta \mu_\beta q_\beta - \omega_\varepsilon \nu_\beta q_2)^2$
	2	$-(\omega_\varepsilon \nu_\beta q_2 - \omega_\alpha \rho_\beta q_\alpha)^2 - (\omega_z \tau_\beta q_z - \omega_\beta \mu_\beta q_\beta - \omega_\varepsilon \nu_\beta q_1)^2$
	3	$-(\omega_\varepsilon \nu_\beta q_1 + \omega_\alpha \rho_\beta q_\alpha)^2 - (\omega_z \tau_\beta q_z + \omega_\beta \mu_\beta q_\beta + \omega_\varepsilon \nu_\beta q_2)^2$
	4	$-(\omega_\varepsilon \nu_\beta q_2 + \omega_\alpha \rho_\beta q_\alpha)^2 - (\omega_z \tau_\beta q_z - \omega_\beta \mu_\beta q_\beta + \omega_\varepsilon \nu_\beta q_1)^2$

where

$$q_1 = \frac{q_x + q_y}{\sqrt{2}}, \quad q_2 = \frac{-q_x + q_y}{\sqrt{2}}, \quad a_\sigma = \Delta + 4E_{JT}^e - 2E_{JT}^\sigma, \quad b = -\Delta + 4E_{JT}^e - 2E_{JT}^z,$$

$$c_\sigma = \sqrt{\frac{a_\sigma}{a_\sigma + b}}, \quad d_\sigma = \sqrt{\frac{b}{a_\sigma + b}}, \quad \eta_z = \frac{4E_{JT}^e}{\Delta + 2E_{JT}^z}, \quad \kappa_\sigma = \frac{4E_{JT}^e}{-\Delta + 2E_{JT}^\sigma}, \quad \lambda_\sigma = \frac{E_{JT}^{\sigma'}}{E_{JT}^\sigma},$$

$$\nu_\sigma = \sqrt{\frac{E_{JT}^e a_\sigma}{E_{JT}^e a_\sigma + E_{JT}^\sigma b}}, \quad \rho_\sigma = \sqrt{\frac{E_{JT}^{\sigma'} b}{E_{JT}^e a_\sigma + E_{JT}^\sigma b}},$$

$$\tau_\sigma = \sqrt{\frac{E_{JT}^e a_\sigma b}{E_{JT}^e (a_\sigma + b)^2}}, \quad \mu_\sigma = \sqrt{\frac{E_{JT}^{\sigma'} a_\sigma b}{E_{JT}^e (a_\sigma + b)^2}}, \quad \nu_\sigma = \frac{a_\sigma - b}{a_\sigma + b},$$

with $\sigma = \alpha$ at $\sigma' = \beta$, and $\sigma = \beta$ at $\sigma' = \alpha$.

For *NJT*-extremum $\varepsilon_0^\sigma = -\Delta - E_{JT}^z$; for *JT $_\sigma$* -extrema points $\varepsilon_0^\sigma = -E_{JT}^\sigma$; for *PJT $_\sigma$* -extrema points $\varepsilon_0^\sigma = -E_{JT}^\sigma - \frac{1}{2}c_\sigma^2 a_\sigma$.

Table 3.

	$a_\sigma < 0$	$a_\sigma > 0$
$b < 0$	<i>NJT</i> + <i>JT$_\sigma$</i>	<i>NJT</i>
$b > 0$	<i>JT$_\sigma$</i>	<i>PJT$_\sigma$</i>

where $a_\sigma = \Delta + 4E_{JT}^e - 2E_{JT}^\sigma$, $b = -\Delta + 4E_{JT}^e - 2E_{JT}^z$.